Science of the Total Environment 691 (2019) 1027–1042

Contents lists available at ScienceDirect

Science of the Total Environment

journal homepage: www.elsevier.com/locate/scitotenv

Inorganic nitrogen wet deposition gradients in the Denver-Boulder metropolitan area and Colorado Front Range – Preliminary implications for Rocky Mountain National Park and interpolated deposition maps

Gregory A. Wetherbee [a,*], Katherine B. Benedict [b], Sheila F. Murphy [a], Emily M. Elliott [c]

[a] U.S. Geological Survey, United States of America
[b] Colorado State University, United States of America
[c] University of Pittsburgh, United States of America

HIGHLIGHTS

- First assessment of reactive inorganic nitrogen wet deposition in the Denver metropolitan area.
- Nitrogen wet deposition varies with land surface elevation and population density.
- Differences in nitrogen sources, transport and deposition evident over urban – montane transect.
- Chemical data and air mass trajectories indicate nitrogen deposition seasonality.
- Urban data improved spatially interpolated N atmospheric deposition maps.

GRAPHICAL ABSTRACT

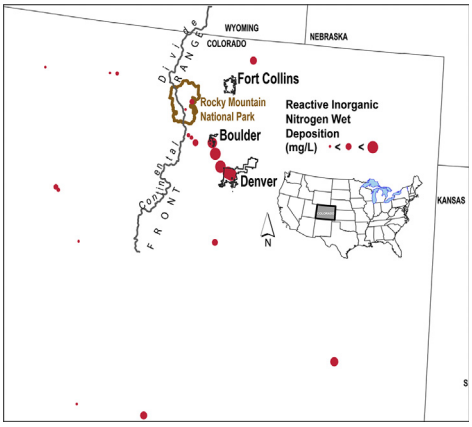

ARTICLE INFO

Article history:
Received 1 April 2019
Received in revised form 28 June 2019
Accepted 30 June 2019
Available online 03 July 2019

Editor: John Walker

Keywords:
Urban atmospheric deposition
Nitrogen
Precipitation
Stable isotopes
Ammonia

ABSTRACT

For the first time in the 40-year history of the National Atmospheric Deposition Program/National Trends Network (NADP/NTN), a unique urban-to-rural transect of wet deposition monitoring stations was operated as part of the NTN in 2017 to quantify reactive inorganic nitrogen wet deposition for adjacent urban and rural, montane regions. The transect of NADP stations (sites) was used to collect continuous precipitation depth and weekly wet-deposition samples in the Denver – Boulder, Colorado, urban corridor. Gradients in reactive inorganic nitrogen (Nr) concentrations and wet deposition were identified along the transect, which included Rocky Mountain National Park. Back trajectory modeling and stable isotopes suggested contribution of agricultural ammonia (NH_3) to urban Nr wet deposition in Denver, but apportionment of wet-deposited Nr to agricultural versus urban mobile sources was not possible for this study. The results demonstrate the importance of multiple monitoring sites across an urban area in defining fine-scale geographic patterns in atmospheric deposition and its sources. Data from new sites located within 50 km of the urban area demonstrate that the urban influence does not extend as far as the inverse distance weighting would have suggested without such empirical

* Corresponding author.
E-mail address: wetherbe@usgs.gov (G.A. Wetherbee).

https://doi.org/10.1016/j.scitotenv.2019.06.528
0048-9697/Published by Elsevier B.V.

Data availability:
Precipitation chemical analysis data for the NUANC sites are available by request to the NADP at http://nadp.slh.wisc.edu/NTN/contacts.aspx. Data for regionally representative NTN sites are available from the NADP web site at http://nadp.slh.wisc.edu/data/NTN/. Precipitation depth records for these sites are available from the NADP at http://nadp.slh.wisc.edu/siteOps/ppt/default.aspx. The stable isotope data are available on the USGS National Water Information System (NWIS, U.S. Geological Survey, 2019) at https://waterdata.usgs.gov/nwis. The ambient ammonia concentration data are available by request to Katherine Benedict, Colorado State University, Department of Atmospheric Science at katherine.benedict@colostate.edu.

monitoring data. It is important to determine the radius of influence of urban emissions and associated deposition on the interpolated deposition raster, which is constrained by a paucity of monitoring sites east of Denver.

Published by Elsevier B.V.

1. Introduction

Characterization of total atmospheric nitrogen deposition in cities is increasing in importance as over 50% of the world's population lives in urban areas with an expected increase to 66% by the year 2050 (United Nations, 2015). Nitrogen deposition in the urban environment affects surface water quality, soil composition, and forest health (Divers et al., 2014; Pouyat et al., 2008). Understanding dry and wet deposition of reactive inorganic nitrogen (Nr) species and other chemical constituents is complicated by the spatial and temporal variability of the many types of emission sources and deposition surfaces in urban areas (Decina et al., 2017; Cook et al., 2018). Urban nitrogen emissions from stationary, mobile, and transient air-pollution sources affect the chemical makeup and physical deposition characteristics of airborne materials, the most important being automobiles (Mage et al., 1996; Mayer, 1999; Bettez and Groffman, 2013; Hamilton et al., 1995; Hofman et al., 2014; Jin et al., 2014; Kirchner et al., 2005; Lovett et al., 2000; Templer and McCann, 2010; Rao et al., 2014).

Wet deposition monitoring by the National Atmospheric Deposition Program (NADP) and ambient air monitoring by the Clean Air Status and Trends Network (CASTNET) purposely avoid urban areas in favor of collecting regionally representative data. Currently, less than 10% of NADP National Trends Network (NTN) monitoring sites are classified as "urban," which are defined as sites within 15 km of an area with a population density exceeding 400 people km^{-2}, and data from these sites are excluded from NADP's interpolated annual wet-deposition map products. For these NADP maps, representative measurements from rural and isolated areas are extrapolated across the entire U.S. landscape, and the urban deposition data are plotted as discrete values that are not incorporated into the interpolated deposition raster. Historically, this approach has been preferred to avoid extrapolation of deposition measurements from urban areas across the non-urban landscape. Consequently, NADP annual wet deposition maps underestimate deposition loads (fluxes) in regions affected by urbanization (Howarth, 2007; Redling et al., 2013; Elliott et al., 2007; Rao et al., 2014; Decina et al., 2017, 2018).

Preferred location selection for both NTN and CASTNET sites has resulted in existing monitoring networks that are strongly influenced by inputs from power plants compared to other sources because elevated smokestacks facilitate the regional transport of emissions (Elliott et al., 2007; Elliott et al., 2009). Despite the effectiveness of existing network sites at monitoring emission reductions stemming from the Clean Air Act and its amendments, there is growing concern that existing network site preferences overlook the single largest emission source in the United States – vehicular emissions, which moreover are emitted closer to the ground and thus are subject to local deposition (Elliott et al., 2007; Elliott et al., 2009; Redling et al., 2013; Fenn et al., 2018). In addition to being sources of dust, transportation is the single largest and most overlooked source of Nr emissions to the atmosphere, accounting for over half of the total nitrogen oxides (NOx) emissions in the eastern United States (Butler et al., 2005; Bettez et al., 2013; Redling et al., 2013). Mobile sources of Nr are also one of the major sources of ammonia (NH_3) emissions, including emissions in Denver (Bishop and Stedman, 2015). Other urban Nr sources include volatilization of NH_3 from fertilizers and sewer gas (Felix et al., 2014). The numerous Nr sources complicated by their spatial distribution and temporal variability makes representative measurement of urban Nr challenging.

A logical step toward better understanding of urban atmospheric deposition across the United States is to increase monitoring in urban areas (Rao et al., 2014). In addition to urban monitoring data, studies are needed to derive proper representation of spatial and temporal variability of urban deposition across different types of urban-rural gradients. This task is commonly achieved through transect studies whereby monitoring sites are located along an urban-rural transect (Bytnerowicz et al., 2015; Padgett et al., 1999; Lovett et al., 2000; Decina et al., 2018, 2017; Rao et al., 2014; Templer and McCann, 2010; Bettez and Groffman, 2013; Cook et al., 2018; Lohse et al., 2008; Hall et al., 2014; Zbieranowski and Aherne, 2012; Sun et al., 2017; Wang et al., 2016; Huang et al., 2015; Li et al., 2013; Pan et al., 2012).

Transect studies indicate pronounced urban-rural gradients in deposition. Rao et al. (2014) characterized urban-rural Nr deposition and its effects in Boston, Massachusetts, and observed more than 100% greater annual Nr deposition load at urban compared to non-urban sites. Recent research throughout the Boston region demonstrates that atmospheric deposition in urban areas is both elevated and highly spatially variable relative to nearby rural ecosystems (Decina et al., 2017). These results indicate that multiple monitoring stations are required within urban areas to accurately characterize the variability of emissions and deposition in these ecosystems and in urban–rural gradients.

This study examines results from the most spatially dense network of NTN sites existing in a metropolitan area. For this effort, six new NTN sites were established in 2017, which added to 15 existing NTN sites in Colorado. In this analysis, chemistry of wet deposition was evaluated for the year (2017) from the new urban sites in the Denver-Boulder, Colorado, metropolitan area (DBM) plus two existing rural, montane sites in the Colorado Front Range, including the Loch Vale, Rocky Mountain National Park site (Fig. S-1). The NADP data were evaluated alongside ambient ammonia monitoring, air mass back trajectory analysis, and nitrate isotopic analysis to further understand deposition loads and sources to urban environments. One of several long-term objectives of this multi-year study is to estimate the contribution of urban N emissions from the DBM to Nr deposition in ROMO. Another objective is to optimize collection and use of urban NADP wet deposition data to

improve spatially interpolated raster calculation for atmospheric wet deposition mapping.

1.1. Study area

Approximately 3.2 million residents live in the DBM study area (MDEDC, 2019). The Denver County population alone was 600,000 residents in 2010 and grew to 705,000 in 2017. The city of Boulder had a population of approximately 108,000 residents in 2018 (U.S. Census Bureau, 2019; Boulder Economics Council, 2019). The urban areas are situated in valleys along the South Platte River basin. Another important feature of the region is a large area of agricultural production northeast of the DBM with approximately 31,500 km^2 of farmland and numerous livestock feed lots (USDA, 2018). The urban, suburban, and agricultural land uses on the eastern side of the study area are contrasted by mostly national forests and wilderness areas located west of the DBM. Consequently, nitrogen (N) emissions are much lower in the Front Range mountains immediately west of the DBM than on the eastern plains, but N is transported into the mountains by infrequent easterly winds (USEPA, 2018; Benedict et al., 2013).

Prevailing winds varied markedly in the DBM during 2017, with strong northeasterly winds dominating in downtown Denver, more westerly winds in the western suburbs, and strong southwesterly winds in Boulder. Montane areas along the Front Range were dominated by westerly winds during the year (Colorado Department of Public Health and Environment (CDPHE), 2018). The climate is characterized by hot and dry summers with scattered convective storms and cool winters with typically moderate, frontal precipitation events (Hanson et al., 1978). Average monthly air temperature in the DBM ranges from approximately 0 °C in winter to 21 °C in summer. The 2017 annual precipitation depth for the DBM was 42 cm (average of five NADP sites) compared to depths of 61 cm and 122 cm for two montane NADP sites located within 48 km of the urbanized areas (NADP, 2018).

The DBM is in the rain shadow of the Rocky Mountains on the Colorado Piedmont along the eastern edge of the Front Range (Hanson et al., 1978). The Front Range generally is the mountainous region between the Arkansas River and the Wyoming State border along the Continental Divide (Trimble and Machette, 1979) (Fig. S-2). The complex topography of the DBM plays a major role in regional air quality with terrain-induced flows and mesoscale circulations, such as easterly weather system flows (upslope) from the Denver Cyclone described by Fried et al. (2016). Air quality impairment occurs in the DBM most often during winter when temperature inversions trap air pollutants in the valleys (Hanson et al., 1978).

Air-pollution emissions data obtained from the 2014 National Emissions Inventory (NEI) for the most populated counties in the region (Denver, Boulder, Jefferson, Douglas, Adams, Arapahoe, Larimer) were estimated at 36,919 metric tons (MT) for nitrogen oxides (NOx) and 916 MT for ammonia (NH_3) from on-road vehicles (USEPA, 2018). Annual NH_3 emissions for fertilizer and non-agriculture vegetation for the counties was 247 MT, and publicly owned treatment works emissions were 0.12 MT in 2014. Livestock emissions for NH_3 were 1195 MT for the urbanized counties, compared to 11,090 MT for agricultural counties with limited urbanization (USEPA, 2018).

The CDPHE Air Pollution Control Division data for 2017 indicate that 66,800 MT of NOx were emitted in the counties with urban areas, approximately half of which is attributed to on-road vehicles per the 2014 NEI (CDPHE, 2018; USEPA, 2018). Approximately 29% of the 2017 NOx emissions in the urbanized counties was from point sources (e.g. electricity generation). Therefore, most of the NOx emissions and half of the NH_3 emissions in the DBM are from vehicles and point sources, but statewide, NH_3 emissions from agricultural sources exceed urban sources by nearly a factor of 10 (Fig. S-3: NOx and NH_3 emissions from biogenic, mobile, and stationary sources in Colorado for 2014 (USEPA, 2018)).

2. Methods and approach

2.1. Network for Urban Atmospheric Nitrogen Chemistry (NUANC)

Six urban wet-deposition monitoring sites were established by the U.S. Geological Survey (USGS) in 2016–2017 as part of the NADP/NTN with support from several cooperators[1] (Fig. S-2). The USGS sites identified as CO87, CO06, CO11, CO86, CO85, and CO84 are the core sites for the Network for Urban Atmospheric Nitrogen Chemistry (NUANC). The CO84 site was added in May 2017 by the Boulder Creek Critical Zone Observatory project, and only a partial record is available for 2017. The locations of these urban sites form a transect across the DBM, which is extended northwest into the mountains of the Colorado Front Range by long-term NADP/NTN sites CO94 and CO98 (Fig. S-2). The CO98 site is located in the Loch Vale watershed in ROMO. The entire transect of eight sites is approximately 90 km long and has an elevation range from 1593 m (Denver) to 3159 m (Loch Vale) above mean sea level (Fig. S-2).

Each monitoring site was equipped with a continuously recording electronic precipitation gage ("gage(s)" hereafter) and a precipitation sample collector ("collector(s)" hereafter, Figs. S-4–S-9). Weekly composite wet-deposition samples were collected every Tuesday unless prevented by inclement weather, in which case samples were collected the next day. Samples residing in the collectors more than 8 days and 2 h were invalidated by NADP. Samples were collected, filtered, and analyzed using NADP protocols (NADP, 2018).

Data for wet-deposition sample concentrations and precipitation depths were obtained from the NADP (NADP, 2018). The wet-deposition data were quality assured and flagged per NADP protocols. Quality rating (QR) codes of "A" and "B" are assigned to data that are usable without restriction, and "C" codes are assigned based on identification of visible contamination in samples with concentrations of at least six analytes above the 95th percentiles for each site's historical record. However, because the six NUANC sites were new, they had no previous records for computation of the 95th percentile concentrations. Therefore, "C"-coded data were used for some aspects of the data analysis as indicated herein.

For security purposes, the urban sites in downtown Denver (CO06 and CO87) were installed on top of 1-story buildings surrounded by other tall buildings and trees. While installing NTN collectors on rooftops violates NADP siting criteria traditionally used for rural sites, it is rarely avoidable in an urban environment. The CO85 site in Boulder was also in violation of siting criteria for multiple objects, including a nearby fence, building, and additional meteorological equipment within 5 to 20 m of the collector. However, violations of siting criteria at these urban sites are hardly unique. Rather, they are similar to many existing NADP sites classified as rural. The NADP siting criteria are not used to invalidate data, but rather to enhance the representativeness of the data for each location. Photographs of the sites are available in the Supplemental Information (Figs. S-4–S-9). Consistency of the data between the urban sites indicated that the configurations of the instruments did not adversely impact 2017 monitoring at any of the sites.

2.2. Stable isotopes in wet deposition

To capture potential variations in sources and formation pathways, the NADP Central Analytical Laboratory (CAL) poured off split samples for stable isotope analyses of natural abundances of nitrogen and oxygen in the nitrate molecules ($\delta^{15}N\text{-}NO_3$ and $\delta^{18}O\text{-}NO_3$, respectively) for weekly samples from February 21–May 23, 2017. Upslope events occur during this period of late winter and spring time when low pressure centers set up southeast of the Continental Divide and push moist

[1] Cooperating entities include:Colorado Department of Public Health and Environment, City and County of Denver, U.S. Fish and Wildlife Service, and University of Colorado-Boulder.

air across the eastern plains and upwards in elevation into the Front Range. Upslope air masses travel over the agricultural and urban areas and move into the mountains. These easterly storm systems move upward in elevation and along the land surface of increasing elevation (orographic lifting) and often cause substantial precipitation. Splits of the weekly-collected composite samples and one discrete upslope event sample (March 29) were filtered with 0.45-μm polyethersulfone filters into 125-mL brown polyethylene bottles with specially sealed caps per NADP protocols, and the samples were frozen to preserve them for isotopic analysis.

After the records for weekly precipitation depth and sample volumes were reviewed, split samples were retrieved from the frozen storage for the March 29 upslope event and weekly composite samples representing upslope and non-upslope conditions. An automated online warning system provided notification of upslope events, but sampling these discrete events was logistically challenging. Composite samples were selected for weeks with the most complete representation throughout the transect of sites.

All of the stable isotope split samples were analyzed for abundance of δ^{15}N-NO_3 and δ^{18}O-NO_3 by the USGS Reston Stable Isotope Laboratory (RSIL). The RSIL standard operating procedures are provided by Coplen et al. (2012). At RSIL, dissolved nitrate in the water was converted to nitrous oxide (N_2O) by denitrifying bacteria that contained a mutation that inhibited the further reduction to N_2, and the N_2O was analyzed for nitrogen and oxygen isotopic abundance by continuous-flow isotope-ratio mass spectrometry (Thermo Scientific Delta V Plus[2] with a universal triple collector). Primary reference materials for δ^{15}N were atmospheric nitrogen gas (N_2), IAEA-N-1, and USGS32, which have assigned values of 0, +0.43 and +180‰, respectively. Primary reference materials for δ^{18}O were Vienna Standard Mean Ocean Water and Standard Light Antarctic Precipitation (SLAP), which have consensus values of 0 and −0755.5‰, respectively, (Coplen et al., 2012).

2.3. Ambient ammonia

Ammonia was measured in the DBM using Radiello radial passive samplers for 2-week integrated samples at three NUANC sites (CO11, CO85, and CO86) and additional Front Range and eastern plains sites, including Denver (La Casa Community Health Center), which is closest to the CO06 NUANC site (Fig. S-2). The ammonia passive sampler includes a blue microporous diffusive body (RAD 1201), an adsorbing cartridge impregnated with phosphoric acid (RAD 168) and a vertical adapter (RAD 122) (Radiello, Padova, Italy). The passive samplers were installed in an inverted bucket to keep direct sunlight, precipitation, and wind from impacting the sampling cartridge (Day et al., 2012). Cartridge extracts from the passive samples were analyzed for ammonium by ion chromatography using 20 millimolar methanesulfonic acid eluent on a Dionex CS12A column followed by a CSRS ULTRA II suppressor and a Dionex CD-20 conductivity detector. To provide context to the urban focused sites, other sites where NH_3 was measured included an agricultural operation (Kersey) and an isolated Front Range site in ROMO.

2.4. Spatial analysis

Annual precipitation-weighted mean concentrations of nitrate (NO_3^-), ammonium (NH_4^+), and Nr were calculated for each monitoring site as:

$$\textit{Annual precipitation weighted mean}\left(Pwm, \frac{mg}{L}\right) = \frac{\sum_{i=1}^{n}(C \times Ppt)}{\sum_{i=1}^{n} Ppt}, \quad (1)$$

where: n is number of weeks with samples, C is concentration of the analyte, in milligrams per liter (mg/L), and Ppt is weekly precipitation, in centimeters (cm). Annual deposition load in kilograms per hectare is calculated as:

$$\textit{Annual deposition load}\ (kg/ha) = Pwm \times Pptyr \times 0.1, \quad (2)$$

where $Pptyr$ is the total precipitation depth for the year irrespective of sample representation, in cm.

Annual precipitation-weighted mean concentrations were mapped for NADP/NTN sites located within 500 km of the DBM, and an interpolated raster was calculated for each analyte with ArcMap Spatial Analyst version 10.5 (Esri, 2016) using cubic inverse distance weighting at a fixed 100-km radius. Each precipitation-weighted mean concentration raster was multiplied by a 4-km^2 raster of 2017 annual precipitation depth obtained from the PRISM Climate Group (URL: http://prism.oregonstate.edu/explorer/, accessed October 24, 2018) to obtain annual wet-deposition load raster maps in units of kilograms per hectare (kg ha^{-1}). This procedure was done for two conditions: 1) including NUANC site data and 2) excluding NUANC site data to evaluate the effects of including urban data in NADP/NTN mapping products.

2.5. Back trajectory modeling

Back trajectory modeling of air masses that generated precipitation for each storm were estimated using the National Oceanic and Atmospheric Administration (NOAA) HYSPLIT model (Stein et al., 2015). The Greenwich Mean Time (GMT) stamps recorded for the start of 15-minute intervals in which the collectors opened for each storm event were used as the start times for 24-hour back trajectory estimation. Back trajectories were estimated for the 500-m, 750-m, and 1000-m altitudes above the land surface for each storm event, and the model was rerun for every 6 h of storm duration. Back trajectory azimuths were estimated manually to the nearest 10 degrees from the monitoring sites back to where the storm air masses were predicted to be in contact with the land surface or to the locations of the air masses at the beginning of the 24-hour period. The back trajectories were precipitation weighted for the weekly composite samples when individual storm back trajectories were within 180 degrees of each other. When storm back trajectories were greater than 180 degrees apart for a composite

Table 1
Median values for weekly ion concentrations in wet-deposition samples from National Atmospheric Deposition Program sites in the Denver-Boulder, Colorado metropolitan area (CO87, CO06, CO11, CO86, CO85, and CO84) and nearby Front Range (CO94 and CO98), 2017.

Analyte	NADP sites in order of increasing latitude, longitude, and elevation along urban-rural transect and decreasing population density							
	CO87	CO06	CO11	CO86	CO85	CO84*	CO94	CO98
	Median values							
Ca^{+2}, mg/L	0.486	0.586	0.528	0.320	0.347	0.257	0.175	0.116
Mg^{+2}, mg/L	0.048	0.062	0.064	0.032	0.042	0.031	0.018	0.013
Na^+, mg/L	0.096	0.162	0.114	0.089	0.067	0.034	0.025	0.013
K^+, mg/L	0.071	0.068	0.067	0.044	0.060	0.045	0.018	0.013
Cl^-, mg/L	0.227	0.343	0.262	0.224	0.193	0.070	0.048	0.03
NH_4^+, mg/L	1.141	1.411	1.267	1.018	1.092	0.771	0.334	0.201
NO_3^-, mg/L	1.562	1.515	1.746	1.502	1.608	1.189	0.700	0.464
N_r, mg/L	1.202	1.427	1.368	1.140	1.218	0.879	0.39	0.246
SO_4^{-2}, mg/L	0.722	1.004	0.806	0.605	0.626	0.406	0.243	0.266
$PctNH_4^+$, (%)	76	78	72	70	70	69	64	59
$PctNO_3^-$, (%)	24	22	28	30	30	31	36	41
H^+, μEq/L	0.339	0.295	0.359	0.525	0.421	0.913	1.698	2.633
pH (from median H)	6.47	6.53	6.44	6.28	6.38	6.04	5.77	5.58
Precipitation, cm	0.66	0.51	0.36	0.72	0.89	0.58	0.79	1.68

[CO84*, partial annual data beginning May 2017; mg/L, milligrams per liter; N_r, reactive inorganic nitrogen; $PctNH_4^+$, percentage of total inorganic nitrogen as ammonium, $PctNO_3^-$, percentage of total inorganic nitrogen as nitrate; (%), percent; H^+, hydrogen ion; cm, centimeters].

[2] Any use of trade, firm, or product names is for descriptive purposes only and does not imply endorsement by the U.S. Government.

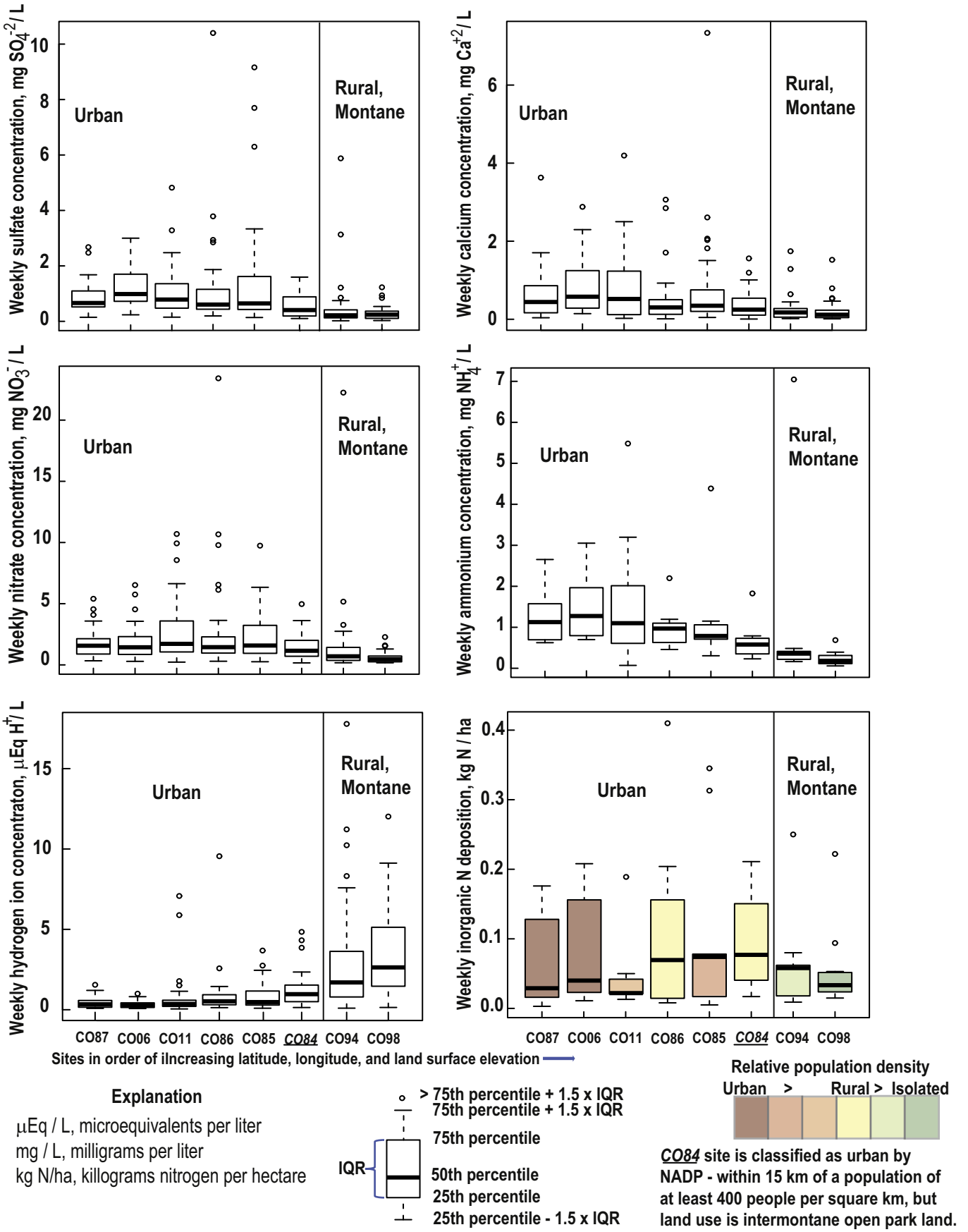

Fig. 1. Concentrations of sulfate, calcium, nitrate, ammonium, hydrogen ion, and reactive inorganic nitrogen deposition load for weekly precipitation samples along an urban to rural, montane transect of sites in the Denver-Boulder metropolitan area and adjacent Front Range mountains, 2017.

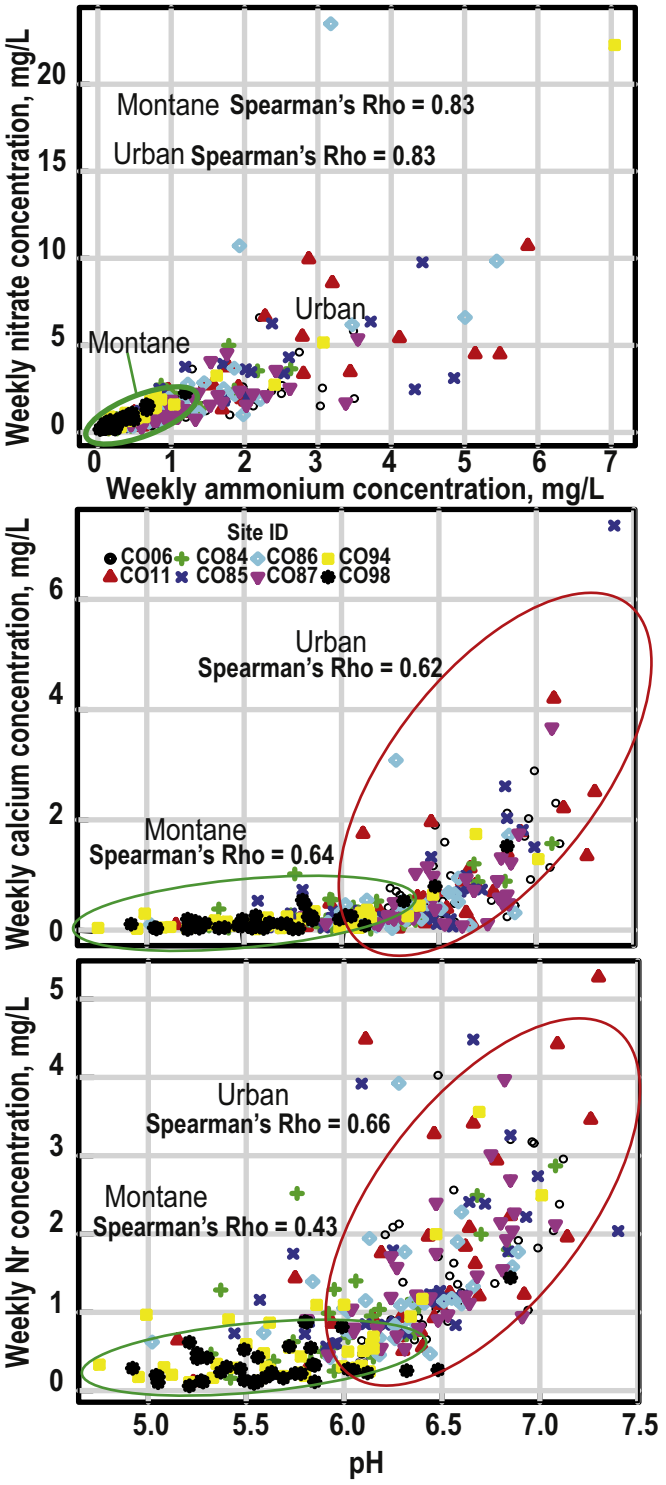

Fig. 2. Weekly nitrate, ammonium, calcium and reactive inorganic nitrogen (Nr) concentrations and pH for National Atmospheric Deposition Program/National Trends Network samples collected along an urban to rural, montane transect of monitoring sites in the Denver-Boulder metropolitan area and Colorado Front Range, 2017.

sample (less than 10% of the samples), the back trajectory azimuths for the storm with the largest amount of precipitation was selected.

The 24-hour back trajectories were used to create weekly concentration rose plots and seasonal deposition-load rose plots (Supplemental Information Fig. S-10) using the "openair" package in R (R Core Team, 2018). The rose plots indicate the dominant regional sectors contributing weekly wet deposited Nr in the wet-deposition samples collected at each site, and also the fraction of Nr as NH_4^+. Isotope rose plots were created to evaluate the $\delta^{15}N\text{-}NO_3$ and $\delta^{18}O\text{-}NO_3$ values with respect to each precipitation event represented by the samples, which were collected for 9 weekly composite periods, and one upslope event on March 29, 2017.

2.6. Statistics

Median and quartile values were calculated for weekly wet-deposition concentration and load measurements. Boxplots of concentrations and loads were plotted using R to illustrate data distributions. Correlation was evaluated with Spearman's Rho (Helsel and Hirsch, 2002).

3. Results

3.1. Reactive inorganic nitrogen deposition in the DBM and front range

Median (50th percentile) values for concentrations of major ions, NH_4^+, NO_3^-, hydrogen (H^+ from pH), Nr, percentages of Nr from both NO_3^- and NH_4^+, and precipitation depth measured at the DBM and rural, montane sites are shown in Table 1. Interquartile range values (75th percentile minus 25th percentile) are shown in Table S-2. Boxplots in Fig. 1 illustrate the data distributions for sulfate (SO_4^{2-}), calcium (Ca^{2+}), NO_3^-, NH_4^+, and H^+ concentrations and Nr wet-deposition load along the transect. Boxplots for magnesium, sodium, potassium, and chloride (not shown) exhibited similar site-specific variability as those in Fig. 1.

Wet-deposition samples from the rural, montane sites, CO94 and CO98, had lower median concentrations for every analyte except H^+ compared to other sites in the transect (Table 1). The rural, montane site concentrations of analytes exhibit smaller interquartile ranges, indicating less variability than urban site concentrations (Fig. 1), except for H^+. Calcium concentrations increase with pH for the urban sites and are highly correlated (Spearman's Rho = 0.62). Calcium concentrations and pH are also highly correlated for the rural, montane sites (Spearman's Rho = 0.64) (Fig. 2). The weekly NO_3^- and NH_4^+ are strongly positively correlated (Spearman's Rho = 0.83) within each urban and rural, montane cluster of data (Fig. 2).

Data shown in Figs. 1 and 3 indicate Nr-concentration and -deposition load gradients along the urban to rural, montane transect of monitoring sites, with higher concentrations and loads in the more intensely urbanized areas (CO87, CO06, CO11, and CO85) compared to less intensely (CO86, CO84) urbanized areas (Fig. 3). Speciation of the components of Nr also changes with distance along the transect. The fraction of annual Nr deposition load from NH_4^+ was 0.77 at CO87 in Denver and decreased to 0.60 at CO98 (Fig. 4), indicating that Nr from NH_4^+ in the wet-deposition samples decreased with distance from the urban corridor and follows a southeast to northwest gradient. As expected, weekly and annual precipitation depths were higher in the mountains than in the DBM (Table 1, Fig. S-11).

Although NO_3^- and NH_4^+ median weekly concentrations are higher in the DBM precipitation than in the mountains, median weekly Nr wet-deposition load measurements are similar in these distinct environments because larger amounts of precipitation fall in the mountains than in the eastern plains, especially in the winter when Nr wet-deposition load was greater at the rural, montane sites than at the DBM sites. Weekly rural, montane Nr wet-deposition loads were comparable and sometimes exceeded urban Nr wet-deposition loads during the late summer (July and September), which also coincided with a period of increased ambient NH_3 concentrations at an agricultural location at Kersey, Colorado, located approximately 45 km northeast of the DBM and 94 km northeast of the CO98 site in ROMO (Fig. 5A).

Measurements of ambient NH_3 in the region's air indicate a strong gradient in ambient NH_3 with higher concentrations in the east to

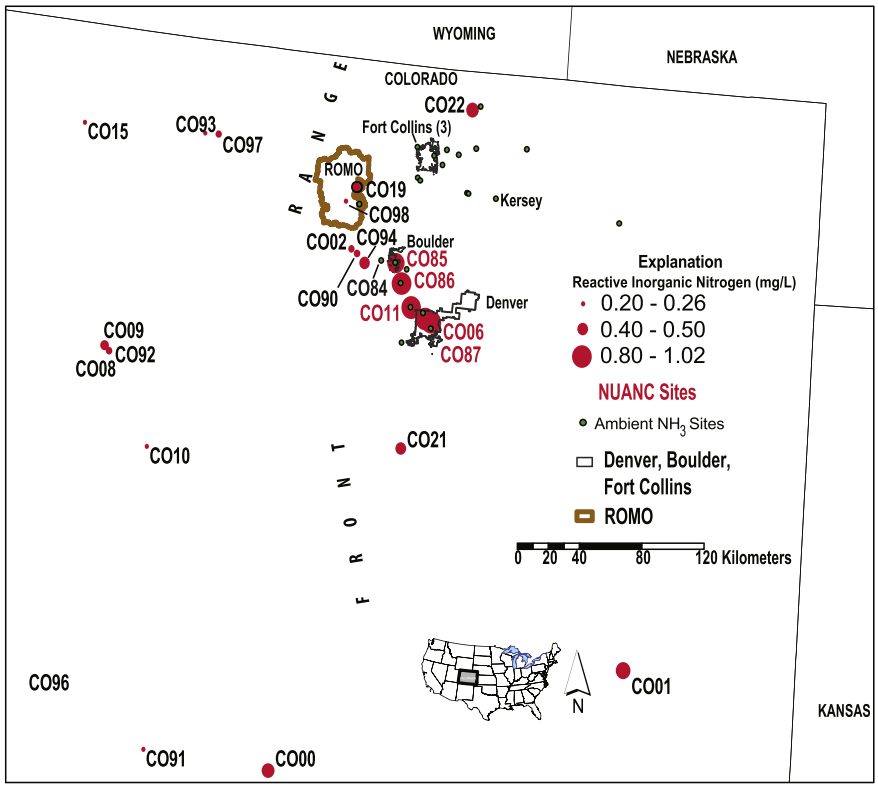

Fig. 3. Annual precipitation-weighted mean reactive inorganic nitrogen concentrations in wet deposition samples for National Atmospheric Deposition Program sites in Colorado, 2017.

lower concentrations in the west, which is consistent with previous measurements by Beem et al. (2010) and Benedict et al. (2013). The trend in concentrations from east to west was observed from downtown Denver to ROMO on average and on a bi-weekly basis (Fig. 5*A*). Ambient concentrations of NH_3 at Kersey are significantly higher than those in Denver by a factor of 12, on average.

Annual wet-deposition loads of NO_3^-, NH_4^+, Nr, SO_4^{-2}, and Ca^{+2} for 2017 are plotted with longitude along the urban-rural, montane transect of NUANC sites in Fig. S-11 (Supplemental Information). Annual NO_3^- load increased between the Denver and Boulder sites across the DBM, and rural, montane loads of approximately 4–5 kg NO_3^- ha^{-1} were similar to the urban site NO_3^- loads. Nr loads decreased from east to west (urban to rural, montane) across the transect (3.9 to 2.9 kg ha^{-1}) largely due to decreasing ammonium loads (3.8 to 2.3 kg ha^{-1}). Loads for SO_4^{-2} and Ca^{+2} ranged from 1.6 to 2.6 kg ha^{-1} and 0.7–1.5 kg ha^{-1}, respectively and varied only slightly across the transect despite the fact that the CO98 site in ROMO received more precipitation than the urban sites by a factor of three.

Rose plots for precipitation depth, Nr concentrations, and fraction of Nr as NH_4^+ indicate that urban sites CO06, CO87 and CO11 had relatively few weekly samples associated with back trajectories from the south and southwest sectors during spring and summer (Fig. 6*a*). Minor Nr contributions from southwesterly storms are evident for the sites CO86 and CO85, in the urban portion of the transect that is closest to the mountains (Fig. 6*a*, *b*). Compared to the urban CO85 site, a slightly larger southwesterly contribution of wet deposition is indicated at site CO94, located 20 km west of CO85 and in the mountains (Fig. 6*b*). By contrast, back trajectories for the CO98 storms were predominantly from the west and southwest sectors, indicating that sources of wet deposition to the CO98 site in ROMO are typically different from those for the other sites in the transect (Fig. 6*b*). Furthermore, the roses plots indicate that the highest percentages of Nr as NH_4^+ occur when storms are northerly, northeastly, and easterly for all sites in the transect except CO98, where samples with the highest percentages of annual Nr as NH_4^+ were from the south, southwest and west.

3.2. Stable isotope composition of wet deposition

The $\delta^{15}N\text{-}NO_3$ values along the transect ranged from −7.99 to 4.51 per mil (‰), and $\delta^{18}O\text{-}NO_3$ values ranged from 49.57 to 77.95‰ with means of −1.98 and 63.88‰ ($n = 56$), respectively. The $\delta^{18}O\text{-}NO_3$ values indicate a gradient along the transect with isotopically lighter $\delta^{18}O\text{-}NO_3$ in the urban precipitation and isotopically heavier $\delta^{18}O\text{-}NO_3$ in the rural, montane precipitation (Fig. 7). Gradients in $\delta^{15}N\text{-}NO_3$ values along the transect occurred as well, but not every week and not always in the same direction along the transect. No gradients in $\delta^{15}N\text{-}NO_3$ values were measured for the weeks ending February 28 through May 9. Then, gradients in $\delta^{15}N\text{-}NO_3$ values were observed for samples collected for the weeks ending May 16 through May 30. The gradient in $\delta^{15}N\text{-}NO_3$ values for the week ending May 16 is in the opposite direction from those observed for the weeks ending May 22 and May 30. The greatest variability in $\delta^{15}N\text{-}NO_3$ values along the transect was observed for an upslope event on March 29, 2017.

The isotope rose plots indicate that isotopically lighter NO_3^- with respect to both $\delta^{15}N\text{-}NO_3$ and $\delta^{18}O\text{-}NO_3$ values is associated with northerly, northeasterly, and easterly storms (Fig. S-12). For urban sites, the isotope rose plots indicate isotopically lighter NO_3^- (44.57–65 (‰ $\delta^{18}O\text{-}NO_3$ and −7.99–1‰ $\delta^{15}N\text{-}NO_3$) was associated with more easterly storms, but heavier isotope ratios (50–77.95‰ $\delta^{18}O\text{-}NO_3$ and −3–4.51‰ $\delta^{15}N\text{-}NO_3$) were found for westerly storms. The CO98 isotope rose plots are markedly different from those of the other sites with most samples having back trajectories from west and southwest sectors. However, CO98 samples with some of the lightest isotope ratios (65.95–68.98‰ $\delta^{18}O\text{-}NO_3$ and −5.88 – −2.21‰ $\delta^{15}N\text{-}NO_3$) were from the southeast and northeast sectors.

3.3. Annual deposition maps

Maps in Fig. 8*A* and *B* compare interpolated Nr wet-deposition load raster data sets to illustrate how inclusion of NADP data from the

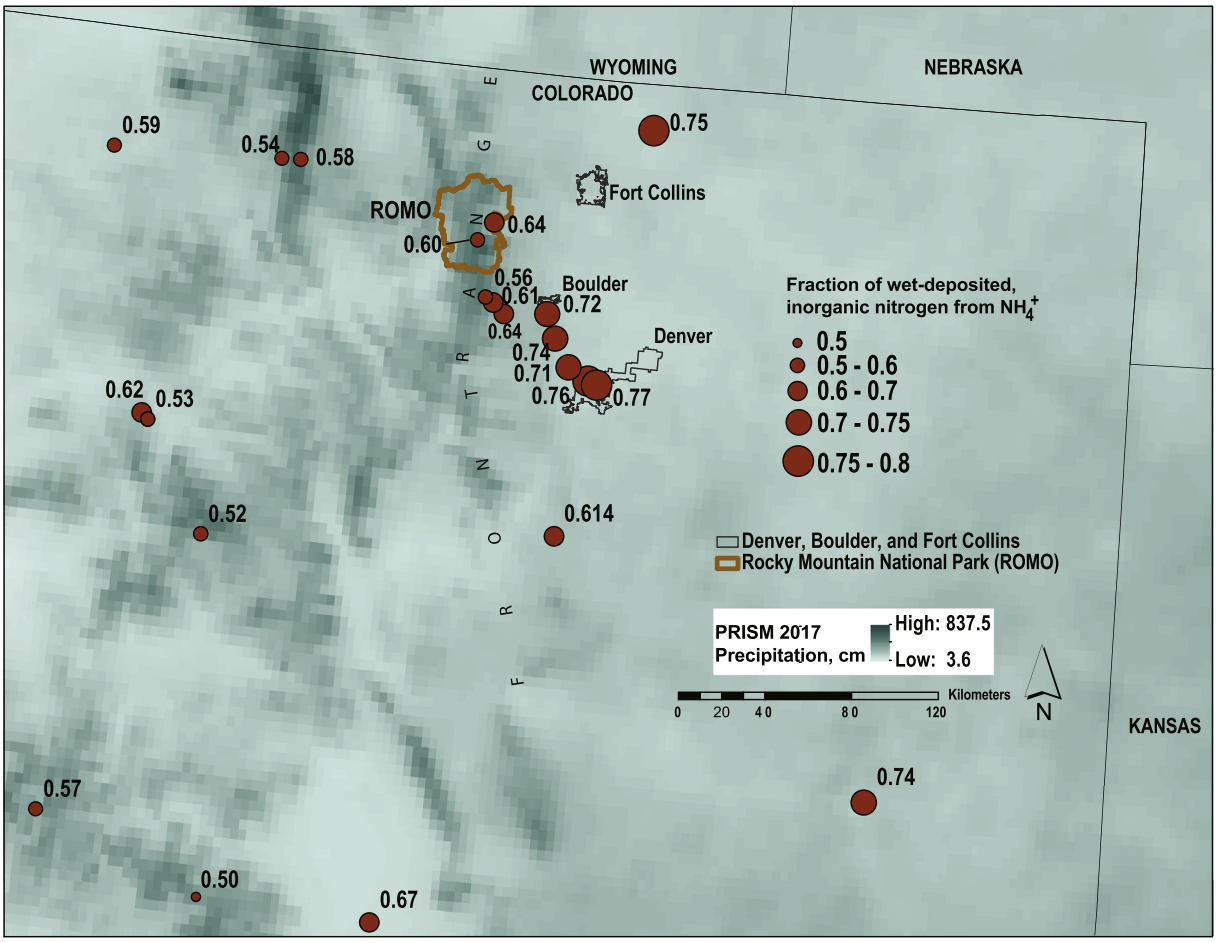

Fig. 4. Fraction of wet-deposited reactive inorganic nitrogen as ammonia (NH_4^+) for National Atmospheric Deposition Program sites in Colorado, and the annual 4-km^2 PRISM precipitation depth raster, 2017 (PRISM Climate Group, 2018).

urban NADP sites in the DBM would change the 2017 NADP annual wet-deposition maps for Colorado. As expected, inclusion of the urban site data increases the estimated Nr wet-deposition load in the DBM region with a radius of influence that extends approximately 100 km outward from Denver (Fig. 8*B*). This is not surprising as a 100-km interpolation radius was used. However, smaller interpolation radii of 50 km and 25 km produced identical raster maps.

The raster in Fig. 8*A* was subtracted from the raster in Fig. 8*B* to obtain the difference raster shown in Fig. 9. A region of Nr wet-deposition load differences between +2 and +3 kg ha^{-1} yr^{-1} are projected beyond 100 km east of the DBM, and differences of approximately +1.5 kg ha^{-1} yr^{-1} are projected northeast into the States of Wyoming and Nebraska. By contrast, there is no measurable difference between the two Nr wet-deposition load raster maps in the Front Range region near ROMO. Data from the montane sites CO94, CO90, CO02, CO98, CO19, and CO21 constrain the urban data interpolation from affecting the Front Range montane region.

The influence of the urban data has unintended effects on the interpolated wet-deposition load raster. The NUANC data coincidentally produced a realistic Nr wet-deposition raster for areas outside the DBM on the eastern plains where agricultural emissions are relatively high, but there are no constraining NADP monitoring sites within that agricultural region to confirm the representativeness of the interpolation. Inclusion of the urban data also resulted in an increase in estimated Nr deposition load for two high-elevation areas approximately 100 km southwest of the DBM (Fig. 8*B*), again with no confirmatory monitoring data for that area.

4. Discussion

4.1. Wet-deposition chemistry in the DBM and Colorado Front Range

The 2017 NUANC provided the first data set for evaluating sources of Nr in the DBM wet deposition, and also for studying the effects of urban air pollution on Nr wet-deposition in the Colorado Front Range. The results, which are consistent with past work by others in several urban settings, demonstrate that urban sites have elevated concentrations and loads of Nr. The urban network of monitoring sites in the DBM allowed identification of concentration and load gradients within a 90-km radius of the DBM and creation of an interpolated map at a finer scale than developed annually by NADP. Together, these findings demonstrate the importance of urban atmospheric deposition monitoring at a finer scale than typically done to quantify and illustrate the influence of urban air pollution on atmospheric wet deposition in the surrounding region.

The data reflect chemical processes and sources of Nr that are characteristic of urban environments. For example, relations of pH with Ca^{+2} and Nr for the urban and montane sites illustrate an example of the urban scrubber phenomenon described by Lovett et al. (2000) whereby dust suspended by urban activity acts as a buffer of acidic wet deposition. The data from this study suggest that dust-induced scrubbing of Nr might also occur. Strong correlation (Spearman's Rho = 0.83) between weekly NO_3^- and NH_4^+ concentrations within each urban and rural, montane cluster of data suggests common sources of both NO_3^- and NH_4^+ within each of these different environments.

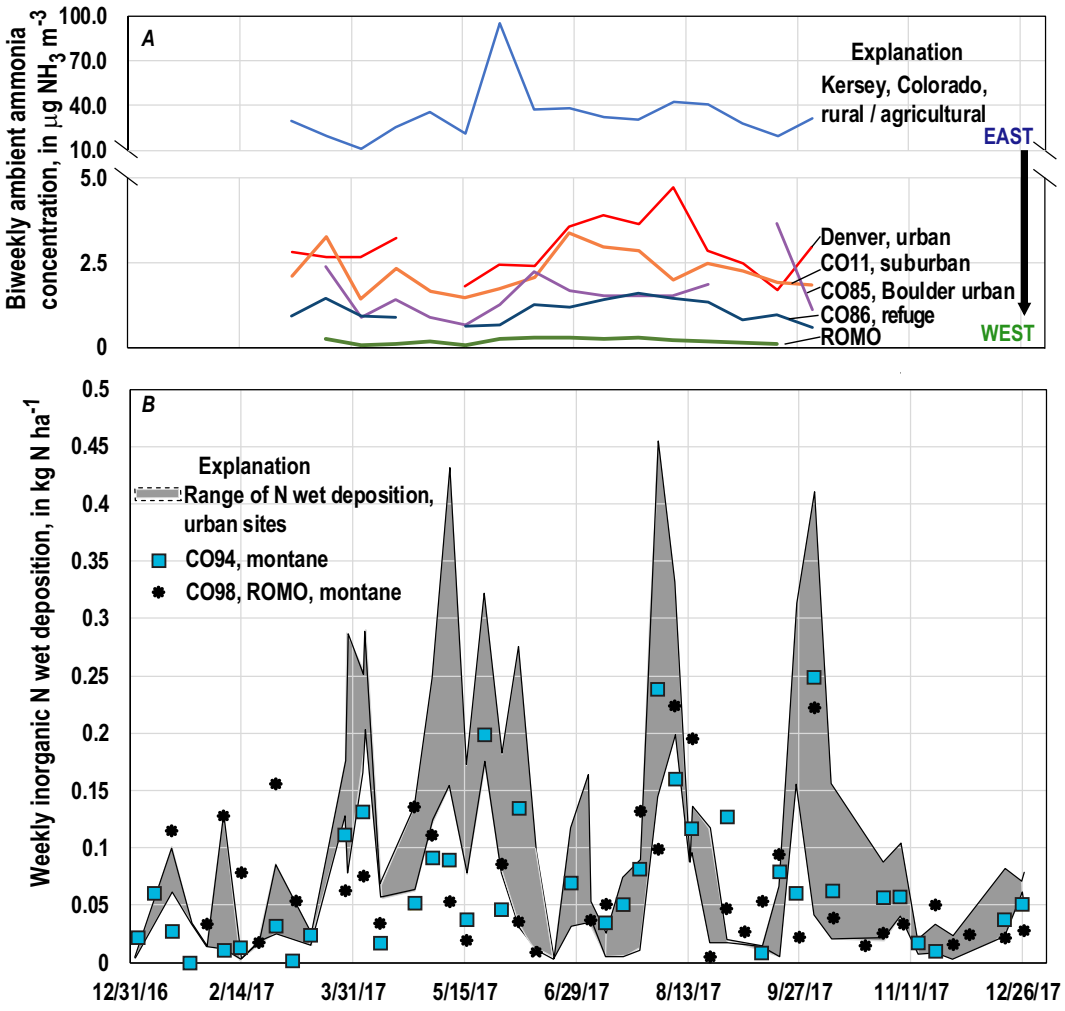

Fig. 5. *A*) Biweekly ammonia concentrations in ambient air in micrograms per cubic meter (μg NH_3 m^{-3}) from passive samplers along a rural-urban-montane gradient, including Rocky Mountain National Park (ROMO) and *B*) weekly reactive inorganic nitrogen (NH_4-N + NO_3-N) wet deposition in kilograms per hectare (kg N ha^{-1}) for National Atmospheric Deposition Program/National Trends Network sites in the Denver-Boulder metropolitan area (6 sites) and montane sites in the Colorado Front Range (2 sites), 2017.

However, the $\delta^{18}O$-NO_3 and $\delta^{15}N$-NO_3 stable isotope data indicate something different - that there are likely different sources of Nr deposition to the DBM region and ROMO, depending on season and storm trajectory (Fig. S-12).

The combination of the time series, back trajectory, and stable isotope data suggest that chemical transformation of the Nr species varied both seasonally and with distance from the DBM. Southeast to northwest gradients of decreasing annual precipitation-weighted mean Nr concentrations along the transect, which coincided with decreasing percentage of total Nr as NH_4^+, indicate that speciation of Nr in the samples also follows the southeast to northwest gradient across the transect. This spatial pattern is consistent with larger sources of NH_3 emissions in the urban and agricultural areas east of the Front Range compared to within the Front Range itself.

Correlations between pH and Nr in urban and montane data clusters suggest that there are differences in Nr sources, atmospheric processing, and deposition processes in the urban and rural, montane environments represented within the transect. Back trajectory modeling results indicated that agricultural NH_3 emitted from the agricultural region north and northeast of Denver might contribute to Nr deposition load in the DBM, but apportionment of NH_4^+ derived from agricultural versus urban NH_3 sources (e.g. livestock, fertilizer versus power generation plants, vehicles) was not possible based on the data obtained during 2017. Decreasing NH_3 concentrations with distance from the urban and agricultural areas suggest a change in source intensity and removal of NH_3 from air masses, by wet and dry deposition, or reaction with particulate matter to form solid phase species such as $(NH_4)_2SO_{4(solid)}$ and $NH_4NO_{3(solid)}$. The patterns suggest that the agricultural region is a source of Nr to the urban area, and that the urban emissions also contribute to episodic Nr wet deposition in the nearby (50 km) Front Range.

The wet-deposition measurements at CO98, in ROMO, were different from those of the other sites in the transect, but not always. Baron and Denning (1993) explain that the uniqueness of CO98 wet-deposition chemistry compared to other Front Range NADP/NTN sites is attributed to the complex topography that prevents air masses from the southeast and east from entering the Loch Vale drainage where site CO98 is located. However, there were several storms sampled at CO98 with greater than 70% of the total Nr as NH_4^+ with back trajectories from the south, southeast, northeast, and northern sectors, suggesting agricultural and minor urban sector contributions of Nr deposition to CO98 for these storms during 2017. Isotope rose plots further indicated that contributions of $\delta^{15}N$-NO_3 from the urban and agricultural regions were larger for CO94 than for CO98 (Fig. S-12). This suggests that sources of NO_3^- in wet deposition at CO94 and CO98 were usually unrelated, and also that sources of NO_3^- in wet deposition at CO98 were usually unrelated to urban emissions in the DBM during 2017.

Some general mechanisms are proposed to explain the atmospheric processing of N in DBM air pollution and observed wet and dry

deposition gradients for upslope (easterly) conditions: 1) gas-particle partitioning of ammonium nitrate (NH_4NO_3) to wet and dry-deposited particles in the dusty urban corridor; 2) denitrification of NO_3^- by NOx and ozone (O_3) to N_2; and 3) dispersion of the urban and agricultural plume(s) as they travel from east to west into higher elevations (Riehl and Herkhof, 1972; Vu et al., 2016; Benedict et al., 2013; Li et al., 2017; Fried et al., 2016). Measurements of other parameters such as: organic nitrogen species; additional stable isotopes (e.g. $\delta^{17}O$-NO_3, ^{15}N-NH_3); washout particulate characterization (e.g. metals, organic carbon, organic nitrogen species, microplastics) and wet- and dry-deposition sampling guided by eddy covariance measurements over a range of atmospheric stability conditions, could improve understanding of emission sources and atmospheric processing of N in the DBM and surrounding agricultural and montane areas (Butler, 1988; Geddes and Murphy, 2014; Johnson et al., 2001; Michalski et al., 2004; Felix et al., 2017).

4.2. Interpolated wet-deposition maps for urban areas

The 2017 NUANC provided the first data set for evaluating the effects of using NADP wet deposition data from urban sites for interpolated atmospheric deposition mapping products. The Nr deposition load differences map illustrates how monitoring data from sites within 50 km of the urban corridor provide realistic constraint on the influence of the

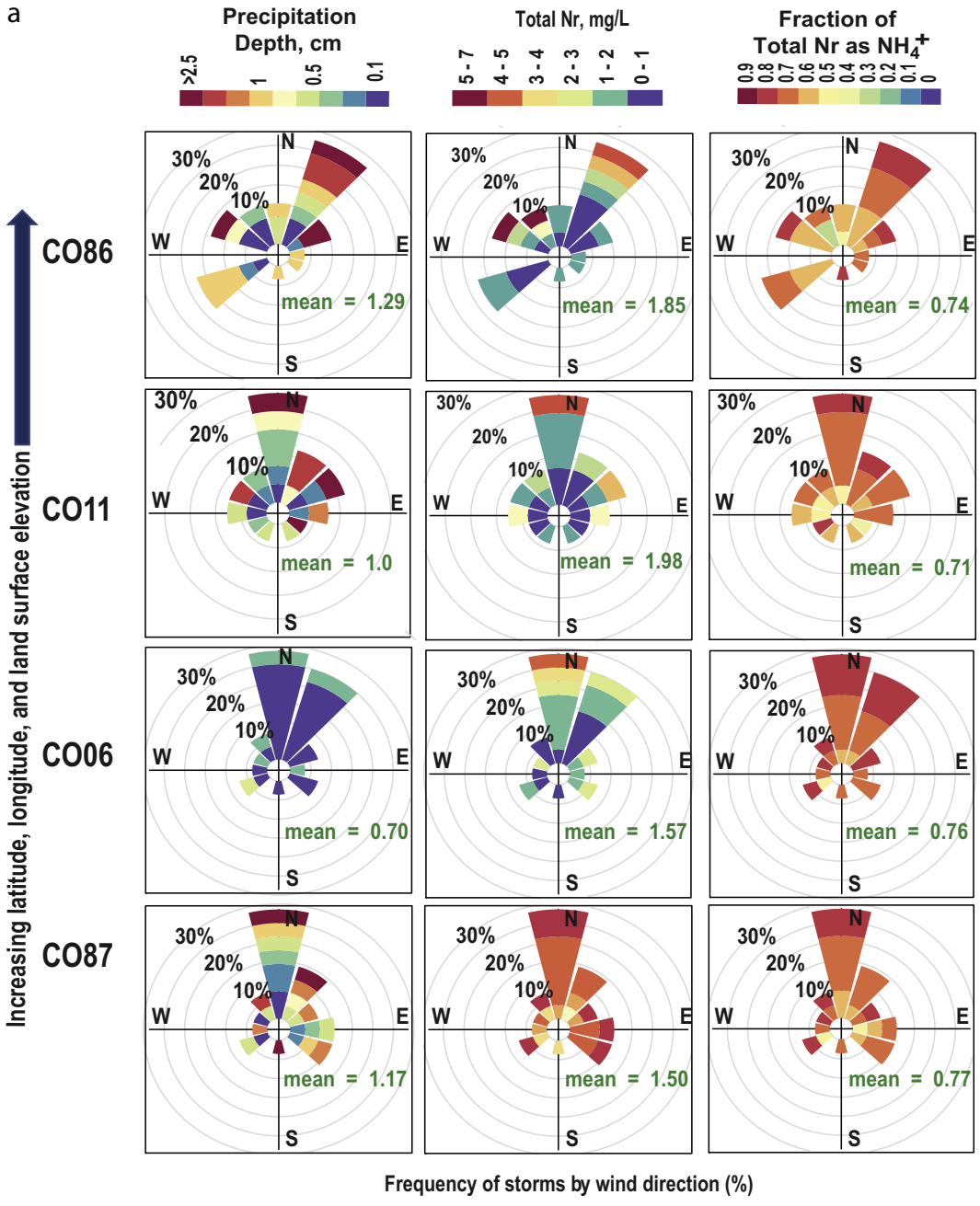

Fig. 6. *a*. Rose plots showing precipitation depth, total reactive inorganic nitrogen (Nr) concentration, and fraction of Nr from ammonium (NH_4^+) plotted by frequency of storms with estimated 24-hour back trajectories in each directional sector for sites in the Denver-Boulder, Colorado metropolitan area, 2017. *b*. Rose plots showing precipitation depth, total reactive inorganic nitrogen (Nr) concentration, and fraction of Nr from ammonium (NH_4^+) plotted by frequency of storms with estimated 24-hour back trajectories in each directional sector for sites in Boulder, Colorado (CO85) and Front Range (CO94, CO98), 2017.

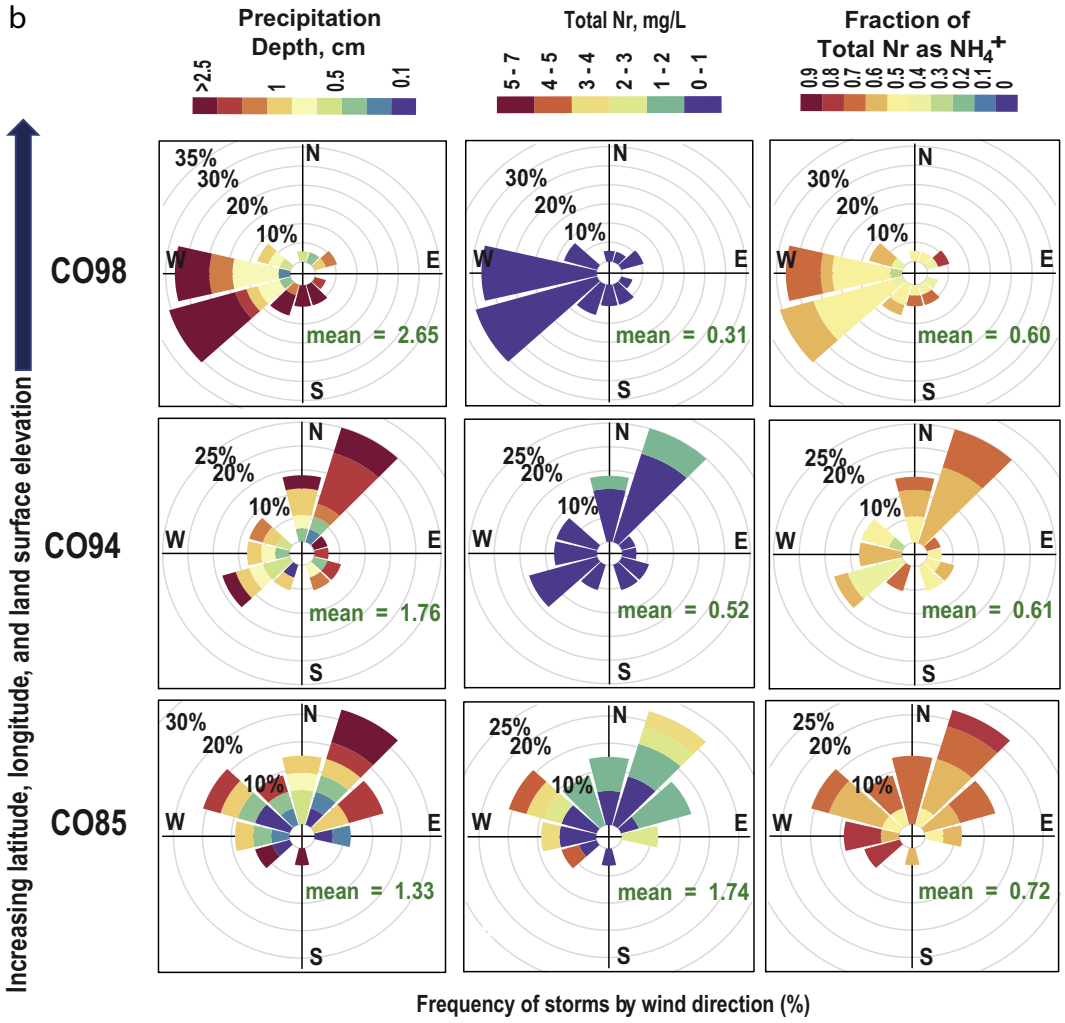

Fig. 6 (*continued*).

urban data in the interpolated raster. The actual radius of influence of the urban site data on the interpolation outside the urban corridor is uncertain and can only be verified with additional monitoring data. For example, the influence of the urban site data on estimated Nr deposition in the ROMO boundary is not detectable from the interpolated raster owing to the spatial control from CO19 and CO98 sites in the park and the nearby rural – isolated, montane CO02, CO90, and CO94 sites.

Inclusion of the 2017 urban data from the NUANC sites in the annual deposition raster likely produces a more representative spatial model of Nr wet deposition for the DBM region. The raster that includes the urban data is much more indicative of the Nr deposition gradient between the urban corridor and mountains to the west. Other North American studies that show similar urban-rural spatial gradients that appear steeper than expected include studies in the San Bernardino Mountains west of Los Angeles, California (Bytnerowicz et al., 2015), Alberta, Canada (Watmough et al., 2014), and Phoenix, Arizona (Cook et al., 2018). The Alberta study used throughfall measurements to show that acid deposition declined logarithmically with distance from the industrial center of their study area, such that sulfur plus nitrogen deposition [load] was substantially reduced within 75 km from the industrial center. In the Phoenix study, Cook et al. (2018) indicated that "regional scale models overestimated deposition [load] rates by 60% …and misidentified hot spots of deposition across the airshed." The Phoenix study area is in an arid airshed with nearby mountainous terrain, which is similar to this study in the DBM area.

In lieu of installing monitoring sites to constrain the urban data-interpolation effect, more work is needed to test algorithms for controlling the radius of influence of the urban data on the interpolated raster. Objective criteria and techniques could be developed to discretize interpolation of basins within the region using land use and topography constraints. Alternatively, the deposition load raster itself could be used to correct the radius of influence. Using the Alberta study (above) as an example, the annual Nr wet deposition measurement from a single urban monitoring site along with calculated, exponentially decreasing Nr values for locations selected radially from the urban center could be used to estimate the Nr deposition load raster for the region, which would include a measured value for the urban center.

5. Conclusions

This study is the first detailed characterization of Nr wet deposition in the DBM, which is complemented by data for ambient ammonia in air and δ^{15}N-NO_3 and δ^{18}O-NO_3 stable isotope data for wet-deposition samples. Monitoring in the urban area improved understanding of N

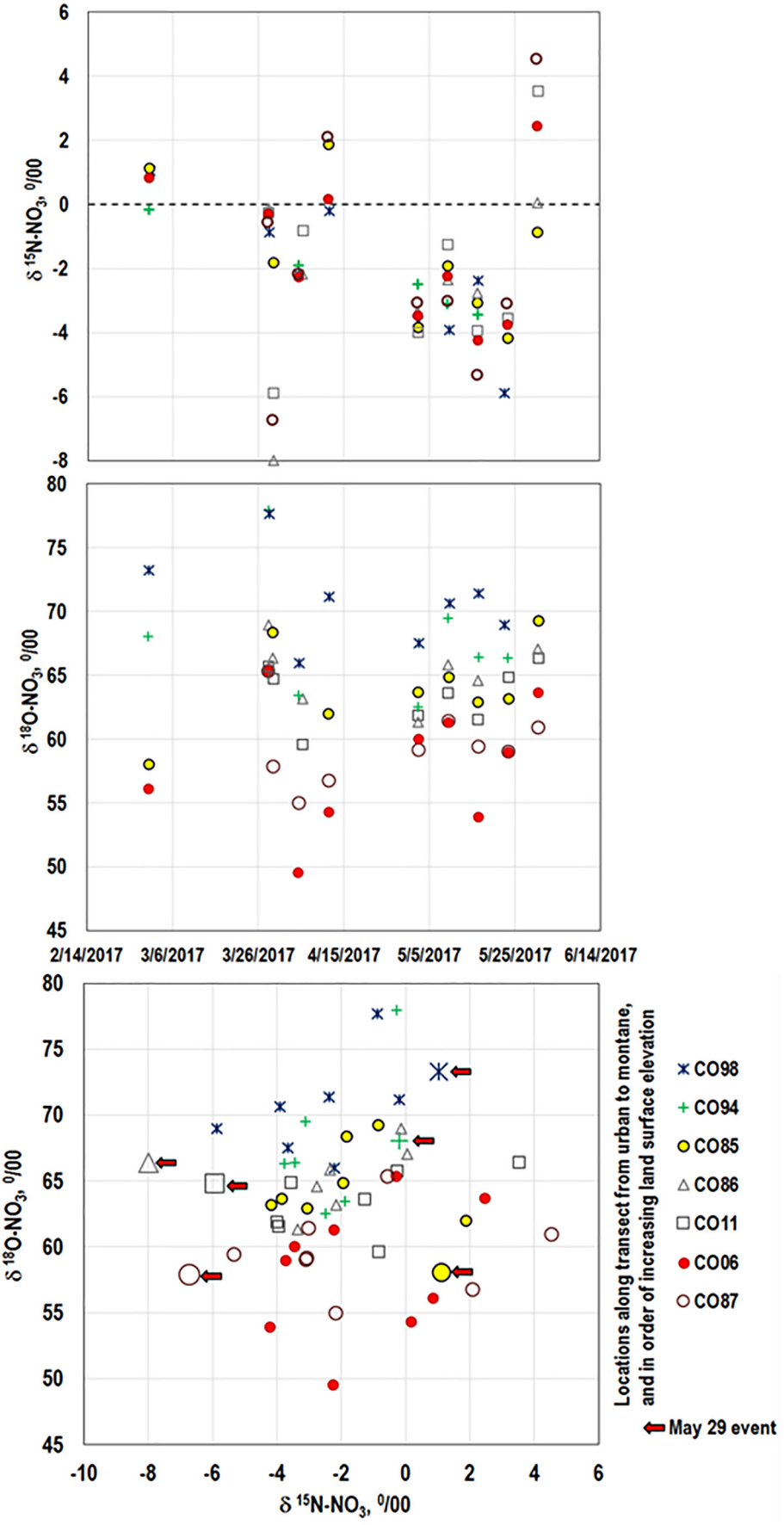

Fig. 7. δ^{15}N-NO_3 and δ^{18}O-NO_3 values (per mil, ^{0}/00) for weekly precipitation samples collected at sites in the Denver-Boulder, Colorado metropolitan area (CO87, CO11, CO86, CO85) and Front Range mountains (CO94, CO98) for 9 weekly composite samples in 2017 and one event sample on March 29, 2017.

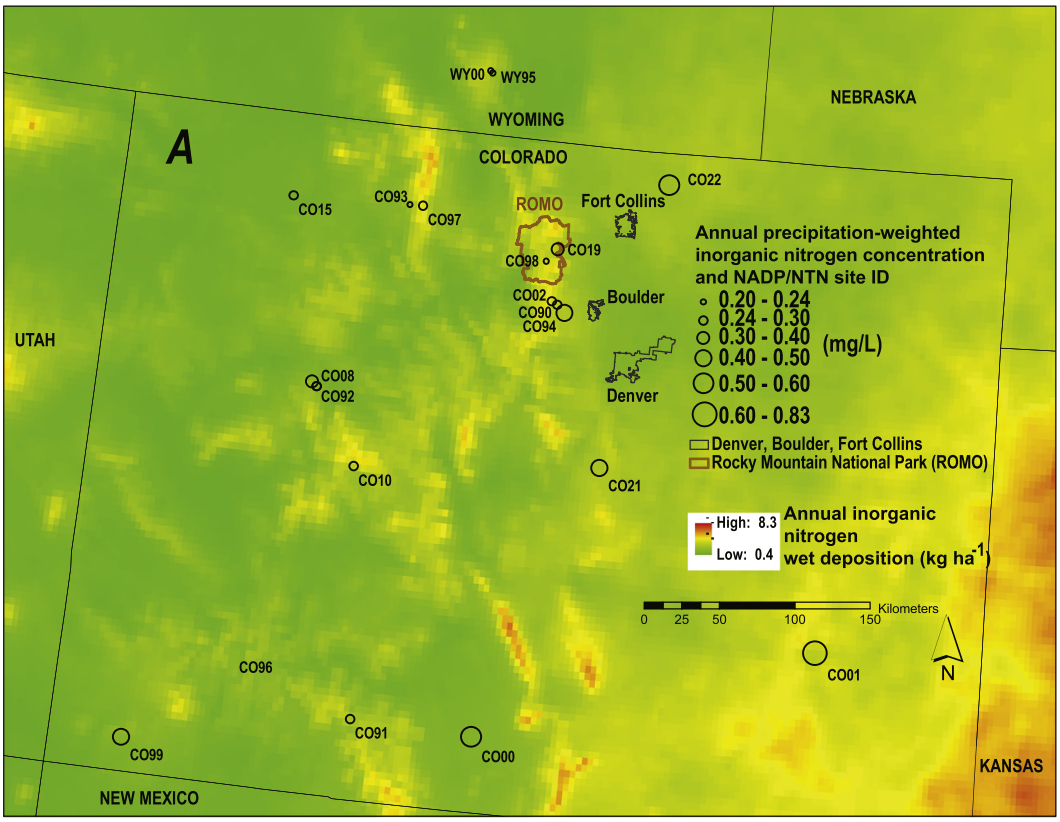

Fig. 8a. *A.* Annual reactive inorganic nitrogen (Nr) precipitation-weighted mean concentrations measured by the National Atmospheric Deposition/National Trends Network (NADP/NTN) sites and estimated Nr wet deposition raster maps interpolated without urban deposition data, 2017. Variation in concentration represented by sizes of circles.

atmospheric deposition loads to the DBM urban environment and outlying region. Wet-deposition Nr and NH_4^+ concentrations and loads decreased with distance from urbanized to non-urbanized (rural, montane) locations along a 90-km transect from the DBM to ROMO, which is also in the same direction of increasing precipitation with increasing land surface elevation. The chemical characteristics of wet deposition and weekly precipitation event trajectories at the CO98 (ROMO) site were markedly different from those at the urban sites for most weekly samples, but not all, suggesting infrequent impacts from DBM air quality on ROMO precipitation quality. Gradients in concentrations of ambient NH_3 in air, Nr (NO_3^- plus NH_4^+) wet deposition, and $\delta^{15}N\text{-}NO_3$ and $\delta^{18}O\text{-}NO_3$ values suggested influences of both agricultural and urban emissions from the eastern plains to both urban and regional Nr deposition, but allocation of specific sources was not possible. The $\delta^{15}N\text{-}NO_3$ and $\delta^{18}O\text{-}NO_3$ values also suggest chemical and phase transformations of Nr species over the urban-rural, montane transect. More work is needed to understand wet-deposition chemical and physical processes specific to urban areas and how sources and transformation of air pollutants affect urban and adjacent environments in the DBM and ROMO.

Urban wet-deposition monitoring improved the spatial representation of interpolated N atmospheric deposition loads for both urbanized and adjacent, non-urbanized areas. Monitoring wet-deposition at locations outside the urban area is essential for controlling the radius of influence of the urban data on interpolated Nr deposition raster data. This study indicated the maximum distance for such monitoring to be less than 20 km (approximate distance between Boulder (CO85) and Sugarloaf (CO94) sites) from the urban corridor, but additional work is needed to determine this distance east of the DBM. Currently, there are 16 sites classified as urban in the entire NADP/NTN nationwide, including the 6 NUANC sites for this study in Colorado. Additional NADP/NTN sites in urban areas are needed nationally to improve the representation of Nr wet-deposition in annual interpolated mapping products.

Funding

Funding for this study was provided by the U.S. Geological Survey National Water Quality Program; Colorado Department of Public Health and Environment Air Pollution Control Division; City and County of Denver Environmental Quality Division; U.S. Fish and Wildlife Service; and The Boulder Creek Critical Zone Observatory. Support was also provided by the U.S. Geological Survey Land Resources Mission Area and NSF grant 1331828: The Boulder Creek Critical Zone Observatory. Additional in-kind support was provided by the University of Colorado at Boulder, Wisconsin Department of Natural Resources, and the USGS Reston Stable Isotope Laboratory.

Acknowledgements

This study was possible due to the collaboration and cooperation of the many people who contributed to the successful operation of the National Atmospheric Deposition Program. Specifically, the authors thank and acknowledge Lisa DeVore, Gregg Thomas, Catherine Collins, Jill Webster, Jack MacDonnell, John Olasin, Pat McGraw, Dillon McClintock-Rager, A. Scott Kittelman, Jill Baron, Daniel Bowker, Jennifer Morse, Tyler Coplen, M. Alisa Mast, RoseAnn Martin, and Amy Ludtke for their help with field operations, data collection and analysis, and chemical analysis of samples.

Appendix A. Supplementary data

Supplementary data to this article can be found online at https://doi.org/10.1016/j.scitotenv.2019.06.528.

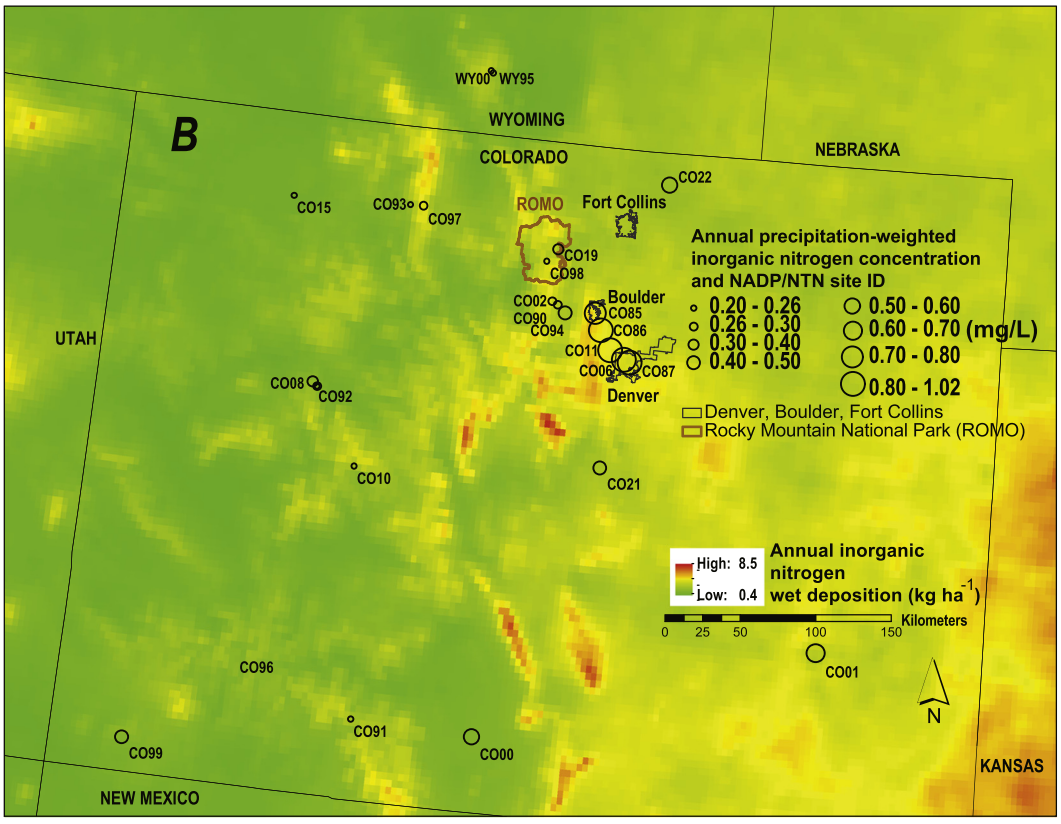

Fig. 8b. *B.* Annual reactive inorganic nitrogen (Nr) precipitation-weighted mean concentrations measured by the National Atmospheric Deposition/National Trends Network (NADP/NTN) sites and estimated Nr wet deposition raster maps interpolated with urban deposition data, 2017. Variation in concentrations represented by sizes of circles.

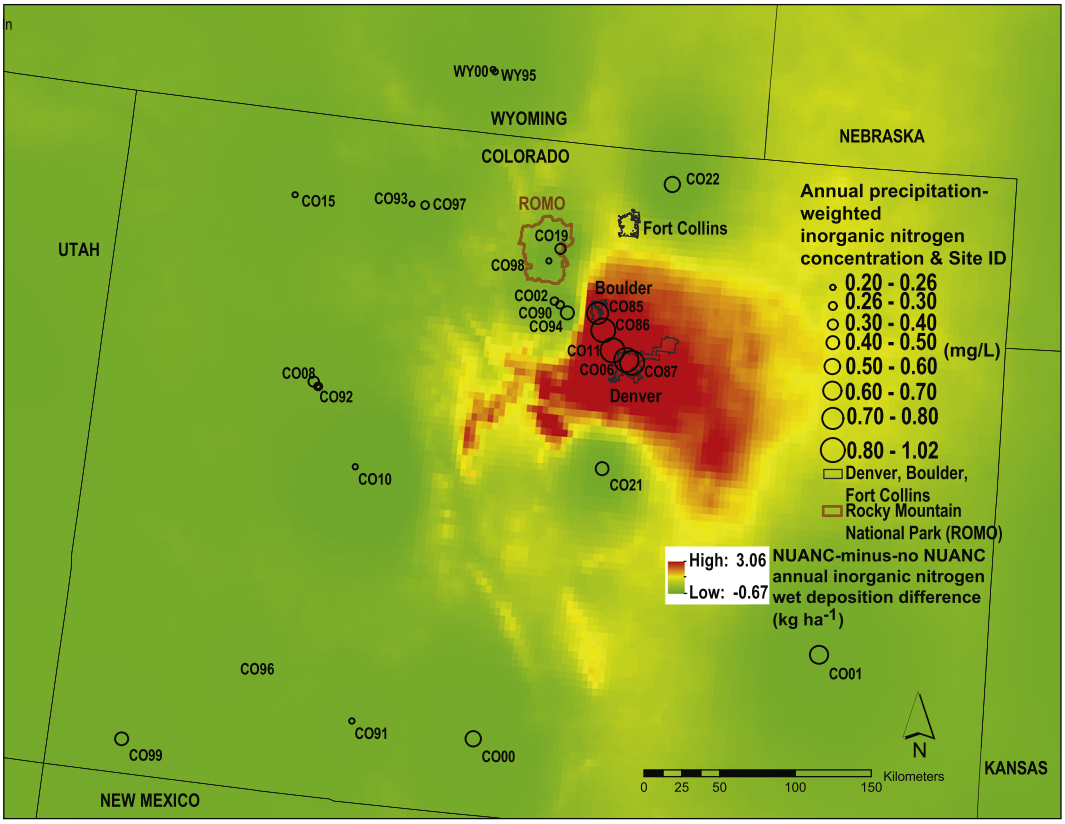

Fig. 9. Annual reactive inorganic nitrogen (Nr) precipitation-weighted mean concentrations measured by the National Atmospheric Deposition/National Trends Network sites and difference between two raster data sets interpolated with and without Network for Urban Atmospheric Nitrogen Chemistry (NUANC) data, 2017. Variation in concentrations represented by sized of circles.

References

Baron, J., Denning, S.A., 1993. The influence of mountain meteorology on precipitation chemistry at low and high elevations of the Colorado Front Range, U.S.A. Atmos. Environ. 27A (15), 2337–2349.

Beem, K.B., Raja, S., Schwandner, F.M., Taylor, C., Lee, T., Sullivan, A.P., Carrico, C.M., McMeeking, G.R., Day, D., Levin, E., Hand, J., Kreidenweis, S.M., Schichtel, B., Malm, W.C., Collett, J.L., 2010. Deposition of reactive nitrogen during the Rocky Mountain Airborne Nitrogen and Sulfur (RoMANS) study. Environ. Pollut. 158, 862–872. https://doi.org/10.1016/j.envpol.2009.09.023.

Benedict, K.B., Day, D., Schwandner, F.M., Kreidenweis, S.M., Schichtel, B., Malm, W.C., Collett, J.L., 2013. Observations of atmospheric reactive nitrogen species in Rocky Mountain National Park and across northern Colorado. Atmos. Environ. 64, 66–76. https://doi.org/10.1016/j.atmosenv.2012.08.066.

Bettez, N.D., Groffman, P.M., 2013. Nitrogen deposition in and near an urban ecosystem. Environ. Sci. Technol. 2013 (47), 6047–6051. https://doi.org/10.1021/es400664b.

Bettez, N.D., Marino, R., Howarth, R.W., Davidson, E.A., 2013. Roads as nitrogen deposition hot spots. Biogeochem 114, 149–163. https://doi.org/10.1007/s10533-013-9847-z.

Bishop, G.A., Stedman, D.H., 2015. Reactive nitrogen species emission trends in three light-/medium-duty United States fleets. Environ. Sci. Technol. 49, 11234–11240. https://doi.org/10.1021/acs.est.5b02392.

Boulder Economic Council, 2019, accessed athttp://boulder economiccouncil.org/boulder-economy/demographic-economic-data/, (February 8, 2019).

Butler, T.J., 1988. Composition of particles dry deposited to an inert surface at Ithaca, New York. Atmos. Environ. 22 (5), 895–900.

Butler, T.J., Likens, G.E., Vermeylen, F.M., Stunder, B.J.B., 2005. The impact of changing nitrogen oxide emissions on wet and dry nitrogen deposition in the northeastern USA. Atmos. Environ. 39, 4851–4862.

Bytnerowicz, A., Johnson, R.F., Zhang, L., Jenerette, G.D., Fenn, M.E., Schilling, S.L., Gonzalez-Fernandez, I., 2015. An empirical inferential method of estimating nitrogen deposition to Mediterranean-type ecosystems: the San Bernardino Mountains case study. Environ. Pollut. 203, 69–88.

Colorado Department of Public Health and Environment (CDPHE), Air Pollution Control Division, 2018. Colorado air quality data report 2017. at. https://www.colorado.gov/airquality/tech_doc_repository.aspx#annual_reports, Accessed date: 13 February 2019.

Cook, E.M., Sponseller, R., Grimm, N.B., Hall, S.J., 2018. Mixed method approach to assess atmospheric nitrogen deposition in arid and semi-arid ecosystems. Environ. Pollut. 239, 617–630.

Coplen, T.B., Qi, H., Révész, K., Casciotti, K., Hannon, J.E., 2012. Determination of the $\delta^{15}N$ and $\delta^{18}O$ of nitrate in water; RSIL lab code 2900, chap. 17 of stable isotope-ratio methods, sec. C of Révész, Kinga, and Coplen, eds. Methods of the Reston Stable Isotope Laboratory (Supersedes Slightly Revised Version 1.0 Released in 2007): U.S. Geological Survey Techniques and Methods book 10, 35 p., available only at. https://pubs.usgs.gov/tm/2006/tm10c17/.

Day, D.E., Chen, X., Gebhart, K.A., Carrico, C.M., Schwandner, F.M., Benedict, K.B., Schichtel, B.A., Collett, J.L., 2012. Spatial and temporal variability of ammonia and other inorganic aerosol species. Atmos. Environ. 61, 490–498. https://doi.org/10.1016/j.atmosenv.2012.06.045.

Decina, S.M., Templer, P.H., Hutyra, L.R., Gately, C.K., Rao, P., 2017. Variability, drivers and effects of atmospheric nitrogen inputs across an urban area; emerging patterns among human activities, the atmosphere and soils, The Sci. Tot. Environ. 609, 1524–1534. https://doi.org/10.1016/j.scitotenv.2017.07.166.

Decina, S.M., Templer, P.H., Hutyra, L.R., 2018. Atmospheric inputs of nitrogen, carbon, and phosphorus across an urban area: unaccounted fluxes and canopy influences. Earth's Future 6, 134–148. https://doi.org/10.1002/2017EF000653.

Divers, M.T., Elliott, E.M., Bain, D.J., 2014. Quantification of nitrate sources to an urban stream using dual nitrate isotopes. Environ. Sci. Technol. 48, 10580–10587. https://doi.org/10.1021/es404880j.

Elliott, E.M., Kendall, C., Boyer, E.W., Burns, D.A., Lear, G.G., Golden, H.E., Halin, K., Bytnerowicz, A., Butler, T.J., Glatz, R., 2009. Dual nitrate isotopes in dry deposition: utility for partitioning NOx source contributions to landscape nitrogen deposition. J. Geophys. Res. 114 (15 p).

Elliott, E.M., Kendall, C., Wankel, S.D., Burns, D.A., Boyer, E.W., Harlin, K., Bain, D.J., Butler, T.J., 2007. Nitrogen isotopes as indicators of NOx source contributions to atmospheric nitrate deposition across the Midwestern and Northeastern United States. Environ. Sci. Technol. 41 (22), 7661–7667. https://doi.org/10.1021/es070898t.

Esri, Inc., 2016. ArcMap 10.5.

Felix, J.D., Elliott, E.M., Gish, T., Maghirang, R., Cambal, L., Clougherty, J., 2014. Examining the transport of ammonia emissions across landscapes using nitrogen isotope ratios. Atmos. Environ. 95, 563–570.

Felix, J.D., Elliott, E.M., Gay, D.A., 2017. Spatial and temporal patterns of nitrogen isotopic composition of ammonia at U.S. ammonia monitoring network sites. Atmos. Environ. 150, 434–442. https://doi.org/10.1016/j.atmosenv.2016.11.039.

Fenn, M.E., Bytnerowicz, A., Schilling, S.L., Vallano, D.M., Zavaleta, E.S., Weiss, S.B., Morozumi, C., Geiser, L.H., Hanks, K., 2018. On-road emissions of ammonia: an underappreciated source of atmospheric nitrogen deposition. Sci. Total Environ. 625, 909–919.

Fried, A., Richter, D., Walega, J., Weibring, P., Vu, K.T., Dingle, J.H., Bahreini, R., Reddy, P.J., Apel, E.C., Campos, T.L., DiGangi, J.P., Diskin, G.S., Herndon, S.C., Hills, A.J., Hornbrook, R.S., Huey, G., Kaser, L., Montzka, D.D., Nowak, J.B., Pusede, S.E., Roscioli, J.R., Sachse, G.W., Shertz, S., Stell, M., Tanner, D., Tyndall, G.S., Weinheimer, A.J., Pfister, G., Flocke, F., 2016. Impacts of the Denver Cyclone on Regional Air Quality and Aerosol Formation in the Colorado Front Range during FRAPPE 2014. Institute of Arctic & Alpine Research Faculty Contributions, p. 9. https://scholar.colorado.edu/instaar_facpapers/9.

Geddes, J.A., Murphy, J.G., 2014. Observations of reactive nitrogen oxide fluxes by eddy covariance above two midlatitude North American mixed hardwood forests. Atmos. Chem. Phys. 14, 2939–2957. https://doi.org/10.5194/acp-14-2939-2014.

Hall, S.J., Maurer, G., Hoch, S.W., Taylor, R., Bowling, D.R., 2014. Impacts of anthropogenic emissions and cold air pools on urban to montane gradients of snowpack ion concentrations in the Wasatch Mountains, Utah. Atmos. Environ. 98, 231–241.

Hamilton, R.S., Revitt, D.M., Vincent, K.J., Butlin, R.N., 1995. Sulphur and nitrogen particulate pollutant deposition on to building surfaces, The Sci. Tot. Environ. 167, 57–66.

Hanson, W.R., Chronic, J., Matelock, J., 1978. Climatography of the Front Range urban corridor and vicinity, Colorado. U.S. Geological Suvey Professional Paper 1019 (59 p).

Helsel, D.R., Hirsch, R.M., 2002. Statistical Methods in Water Resources, Techniques of Water-Resources Investigations of the United States Geological Survey, Book 4, Hydrologic Analysis and Interpretation, Chapter A3 (510 p).

Hofman, J., Bartholomeus, H., Calders, K., Van Wittenberghe, S., Wuyts, K., Samson, R., 2014. On the relation between tree crown morphology and particulate matter deposition on urban tree leaves: a ground-based LiDAR approach. Atmos. Environ. 99, 130–139.

Howarth, R.W., 2007. Atmospheric deposition and nitrogen pollution in coastal marine ecosystems. Acid in the Environment. Springer U.S, pp. 97–116.

Huang, J., Zhang, W., Zhu, X., Gilliam, F.S., Chen, H., Lu, X., Mo, J., 2015. Urbanization in China changes the composition and main sources of wet inorganic nitrogen deposition. Environ. Sci. Pollut. Res. 22, 6526–6534. https://doi.org/10.1007/s11356-014-3786-7.

Jin, S., Guo, J., Wheeler, S., Shengquan Che, L.K., 2014. Evaluation of impacts of trees on PM2.5 dispersion in urban streets. Atmos. Environ. 99, 277–287.

Johnson, C.A., Mast, M.A., Kester, C.L., 2001. Use of $^{17}O/^{16}O$ to trace atmospherically-deposited sulfate in surface waters: a case study in alpine watersheds in the Rocky Mountains. Geophys. Res. Lett. 28 (23), 4483–4486.

Kirchner, M., Jakobia, G., Feichta, E., Bernhardtb, M., Fischer, A., 2005. Elevated NH_3 and NO_2 air concentrations and nitrogen deposition rates in the vicinity of a highway in southern Bavaria. Atmos. Environ. 39, 4531–4542.

Li, K., Liu, X., Song, W., Chang, Y., Hu, Y., Tian, C., 2013. Atmospheric nitrogen deposition at two sites in an arid environment of Central Asia. PLoS One 8 (6), e67018. https://doi.org/10.1371/journal.pone.0067018.

Li, Y., Thompson, T.M., Van Damme, M., Chen, X., Benedict, K.B., Shao, Y., Day, D., Boris, A., Sullivan, A.P., Ham, J., Whitburn, S., Clarisse, L., Coheur, P.-F., Collett Jr., J.L., 2017. Temporal and spatial variability of ammonia in urban and agricultural regions of northern Colorado, United States. Atmos. Chem. Phys. 17, 6197–6213. doi:https://doi.org/10.5194/acp-17-6197-2017.

Lohse, K.A., Hope, D., Sponseller, R., Allen, J.O., Grimm, N.B., 2008. Atmospheric deposition of carbon and nutrients across an arid metropolitan area. Sci. Tot. Environ. 402, 95–105.

Lovett, G.M., Traynor, M.M., Pouyat, R.V., Carreiro, M.M., Zhu, W.-X., Baxter, J.W., 2000. Atmospheric deposition to oak forests along an urban-rural gradient. Environ. Sci. Technol. 34, 4294–4300.

Mage, D., Ozonlins, G., Peterson, P., Webster, A., Orthofer, R., Vandeweerd, V., Gwynne, M., 1996. Urban air pollution in megacities of the world. Atmos. Environ. 30 (5), 681–686.

Mayer, H., 1999. Air pollution in cities. Atmos. Environ. 33, 4029–4037.

Metro Denver Economic Development Corporation (MDEDC), 2019. . accessed at. http://www.metrodenver.org/do-business/demographics/ (February 8, 2019).

Michalski, G., Bohlke, J.K., Thiemens, M., 2004. Long term atmospheric deposition as the source of nitrate and other salts in the Atacama Desert, Chile: new evidence from mass-independent oxygen isotopic compositions. Geochemica et Cosmochmica Acta 68 (20), 4023–4038. https://doi.org/10.1016/j.gca.2004.04.009.

National Atmospheric Deposition Program (NADP), 2018. USDA National Institute of Food and Agriculture National Research Support Project (NRSP-3); NADP Program Office, Wisconsin State Laboratory of Hygiene,465 Henry Mall. University of Wisconsin, Madison,WI 53706 http://nadp.slh.wisc.edu/data/NTN/.

NWIS, U.S. Geological Survey, 2019. USGS Water Data for the Nation. https://waterdata.usgs.gov/nwis.

Padgett, P.E., Allen, E.B., Bytnerowicz, A., Minich, R.A., 1999. Changes in soil inorganic nitrogen as related to atmospheric nitrogenous pollutants in southern California. Atmos. Environ. 33, 769–781.

Pan, Y.P., Wang, Y.S., Tang, G.Q., Wa, D., 2012. Wet and dry deposition of atmospheric nitrogen at ten sites in Northern China. Atmos. Chem. Phys. 12, 6515–6535. https://doi.org/10.5194/acp-12-6515-2012.

Pouyat, R.V., Yesilonis, I.D., Szlavecz, K., Csuzdi, C., Hornung, E., Korsós, Z., Russell-Anelli, J., Giorgio, V., 2008. Response of forest soil properties to urbanization gradients in three metropolitan areas. Landsc. Ecol. 23, 1187–1203. https://doi.org/10.1007/s10980-008-9288-6.

PRISM Climate Group, Oregon State University, http://prism.oregonstate.edu, created October 24, 2018.

R Core Team, 2018. R: A Language and Environment for Statistical Computing, Version 3.5.2. R Foundation for Statistical Computing https://www.R-project.org.

Rao, P., Hutyra, L.R., Raciti, S.M., Templer, P.H., 2014. Atmospheric nitrogen inputs and losses along an urbanization gradient from Boston to Harvard Forest, MA. Biogeochem 121, 229–245. https://doi.org/10.1007/s10533-013-9861-1.

Redling, K., Elliott, E., Bain, D., Sherwell, J., 2013. Highway contributions to reactive nitrogen deposition: tracing the fate of vehicular NOx using stable isotopes and plant biomonitors. Biogeochem 116, 261–274.

Riehl, H., Herkhof, D., 1972. Some aspects of Denver Air Pollution Meteorology. J. App. Met. 11, 1040–1047.

Stein, A.F., Draxler, R.R., Rolph, G.D., Stunder, B.J.B., Cohen, M.D., Ngan, F., 2015. NOAA's HYSPLIT atmospheric transport and dispersion modeling system. Bull. Amer. Meteor. Soc. 96, 2059–2077. https://doi.org/10.1175/BAMS-D-14-00110.1.

Sun, K., Tao, L., Miller, D.J., Pan, D., Golston, L.M., Zondlo, M.A., Griffin, R.J., Wallace, H.W., Jun, Y.J., Leong, Yang, M.M., Zhang, Y., Mauzerall, D.L., Zhu, T., 2017. Vehicle emissions as an important urban ammonia source in the United States and China. Environ. Sci. Technol. 51, 2472–2481. https://doi.org/10.1021/acs.est.6b02805.

Templer, P.H., McCann, T.M., 2010. Effects of the hemlock woolly adelgid on nitrogen losses from urban and rural northern forest ecosystems. Ecosystems 13, 1215–1226.

Trimble, D.E. and Machette, M.N., 1979, Geologic Map of the Greater Denver Area, Front Range urban corridor, Colorado, DOI:https://doi.org/10.3133/i856H, accessed February 11, 2019 at: https://pubs.er.usgs.gov/publication/i856H.

U.S. Census Bureau, 2019. accessed at. https://www.census.gov/quickfacts/denvercountycolorado (February 8, 2019).

United Nations, 2015. World Urbanization Prospects, the 2014 Revision, ST/ESA/SER.A/366. New York. p. xxi.

USDA, National Agricultural Statistics Service, 2018. Census of Agriculture, 2012 State and County Profiles-Colorado. at. https://www.nass.usda.gov/Publications/AgCensus/2012/Online_Resources/County_Profiles/Colorado/index.php, Accessed date: 13 February 2019.

USEPA, 2018. 2018 national emissions inventory, version 2 technical support document. Research Triangle Park, North Carolina, Accessed date: 13 February 2019 at:. https://www.epa.gov/air-emissions-inventories/2014-national-emissions-inventory-nei-data.

Vu, K.T., Dingle, J.H., Bahreini, R., Reddy, P.J., Apel, E.C., Campos, T.L., DiGangi, J.P., Diskin, G.S., Fried, A., Herndon, S.C., Hills, A.J., Hornbrook, R.S., Huey, G., Kaser, L., Montzka, D.D., Nowak, J.B., Pusede, S.E., Richter, D., Roscioli, J.R., Sachse, G.W., Shertz, S., Stell, M., Tanner, D., Tyndall, G.S., Walega, J., Weibring, P., Weinheimer, A.J., Pfister, G., Flocke, F., 2016. Impacts of the Denver Cyclone on regional air quality and aerosol formation in the Colorado Front Range during FRAPPÉ 2014. Atmos. Chem. Phys. 16, 12039–12058. https://doi.org/10.5194/acp-16-12039-2016.

Wang, H., Yang, R., Shi, G., Tian, M., Zhang, L., Zhang, L., Fu, C., 2016. Ambient concentration and dry deposition of major inorganic nitrogen species at two urban sites in Sichuan Basin, China. Envrion. Pollut. 219, 235–244.

Watmough, S.A., Whitfield, C.J., Fenn, M.E., 2014. The importance of atmospheric base cation deposition for preventing soil acidification in the Athabasca Oil Sands Region of Canada. Sci. Tot. Environ. 493, 1–11.

Zbieranowski, A.L., Aherne, J., 2012. Ambient concentrations of atmospheric ammonia, nitrogen dioxide and nitric acid across a rural –urban-agricultural transect in southern Ontario, Canada. Atmos. Environ. 62, 481–491.